Acta Cryst. (1996). B52, 586–595

Ab Initio Hartree–Fock Study of the Electronic Charge Density of the Cubic Boron Nitride and its Comparison with Experiments

ALBERT LICHANOT,[a]* PATRICK AZAVANT[a] AND ULLRICH PIETSCH[b]

[a]*Laboratoire de Chimie Structurale, Université de Pau et des Pays de l'Adour, URA 474, IFR, Rue Jules Ferry 64000 Pau, France, and* [b]*Institute of Solid State Physics, University of Potsdam, D14415 Potsdam, Germany*

(*Received 22 November 1995; accepted 22 February 1996*)

Abstract

The electronic charge density of cubic boron nitride is calculated within the *ab initio* Hartree–Fock approximation using the program *CRYSTAL*. Based on Debye hypothesis, the thermal motion of atoms is considered by disturbing the atomic orbitals by mean-square displacements given from experiment. The calculated difference charge density obtained by subtraction of the total density and that of an independent atomic model (IAM) is characterized by a charge-density accumulation between next neighbours slightly shifted towards the nitrogen. The calculated X-ray structure amplitudes are compared with two different data sets [Josten (1985). Thesis. University of Bonn, Germany; Eichhorn, Kirfel, Grochowski & Serda (1991). *Acta Cryst.* B47, 843–848]. In both cases, very good agreement is found beyond the 420 reflection. The first six structure amplitudes are generally lower or larger compared with Josten's and Eichhorn *et al.*'s data, respectively. Whereas our charge density can be interpreted by a balanced ratio between covalent overlap and electronic charge transfer between neighbouring valence shells, the density plots calculated from experimental data express either the charge transfer (Josten, 1985) or the covalency (Eichorn *et al.*, 1991).

1. Introduction

Boron nitride is usually found in the graphite-like phase, but its zinc blende structure phase was synthesized *ca* 40 years ago for the first time (Wentorf, 1957). This cubic boron nitride (c-BN) is diamond-like, but the space-group symmetry is changed from the centrosymmetric F_{d3m} of diamond to the non-centrosymmetric $F_{\bar{4}3m}$ group for c-BN. As with numerous boron compounds, c-BN has a high melting point and a very large hardness (Brookes, Hooper & Lambert, 1983), and is also characterized by a high thermal conductivity. This is expressed by a bulk modulus of 420–430 GPa (Orlando, Dovesi, Roetti & Saunders, 1990) and a Debye characteristic temperature of 1600 K (Atake, Takai, Honda, Saito & Saito, 1991), which are slightly smaller than those of diamond [460–470 GPa (Orlando *et al.*, 1990) and 1850 K (Atake *et al.*, 1991), respectively]. To understand the similarities of these properties, it is mostly interesting to know the charge density of c-BN and to compare it with that of diamond, which has been studied theoretically (Orlando *et al.*, 1990; Spackman, 1991) and experimentally (Spackman, 1991; Takama, Tsuchiya, Kobayashi & Sato, 1990). Both diamond and c-BN are made of atoms belonging to the first row of the periodic table: they are isoelectronic compounds and can be considered as model systems of the elemental IV and III–V group semiconductors. The charge densities of these compounds have been parametrized recently by one of us (Pietsch, 1985) in order to study the structure-to-property connections. The energy gap between the conduction and valence band levels varies as a function of the overlap charge transfer between next-nearest neighbours, for instance. However, a critical comparison of theoretical (Cohen & Chelikowsky, 1989) and experimental charge densities reveals some disagreements. They may be due either to the different levels of approximation within the theoretical frameworks or to the various corrections of experimental X-ray structure amplitudes, which are necessary to construct the charge density. This concerns the spatial shape of the bond charge and the amount of electronic charge transfer between next neighbours. As an example, the c-BN represents one of the simplest III–V compounds, which enables an instructive study of these properties.

From the experimental point of view, the charge density of c-BN is known from the X-ray structure factors measured by Weiss (1974) or more recently by Josten (1985), Will, Kirfel & Josten (1986) and Eichhorn *et al.* (1991). Whereas the charge density constructed from Josten's (1985) data is characterized by a large electron concentration close to the N atom, Eichhorn *et al.*'s (1991) data show a pronounced charge-density maximum between next-nearest neighbours.

Similar discrepancies are obtained from two theoretical studies made by means of the *ab initio* Hartree–Fock method (Orlando *et al.*, 1990; Euwema, Surratt, Wilhite & Wepfer, 1974). In the first study (Orlando *et al.*, 1990) the bond charge in the electron charge-density map appears to be almost similar to diamond, but is localized closer to the anion site, and the charge

transfer deduced from a Mulliken population analysis is 0.86 e. The structure factors corresponding to nine valence reflections are calculated in the second study (Euwema *et al.*, 1974) and the high value of that associated with the 200 reflection indicates a large charge transfer between B and N atoms.

In the present work the same *ab initio* Hartree–Fock methodology as that presented by Orlando *et al.* (1990) was used. The experimental geometry (lattice parameter $a = 3.615$ Å) is adopted to allow an accurate comparison with experiment. Different atomic orbital basis sets describing B and N atoms, without and with polarization functions, are variationally optimized with respect to this geometry. Discussions are made on the basis set effects and better physical properties can be obtained. The structure factors and the charge density are calculated from the static and dynamic ($T = 298$ K) cases and compared with the corresponding experimental values measured by Josten (1985) and Eichhorn *et al.* (1991). The temperature effect on the electron charge distribution is also analysed.

2. Computational procedure and basis set description

A crystalline wavefunction calculation was performed with the *CRYSTAL* code, available at the QCPE [Quantum Chemistry Program Exchange (Dovesi, Pisani, Roetti, Causà & Saunders, 1989; Dovesi, Roetti & Saunders, 1992)] and which is distributed worldwide now. An exhaustive description of the periodic Hartree–Fock crystalline orbital self-consistent field (SCF) computational scheme embodied in this program is available elsewhere (Pisani, Dovesi & Roetti, 1988).

The evaluation of the Coulomb and exchange series is carried out by adopting the following values of truncation tolerances, $ITOL_1 = ITOL_2 = ITOL_3 = 5$, $ITOL_4 = 6$, $ITOL_5 = 12$. These values indicate that the two centre integrals are disregarded or neglected (Pisani *et al.*, 1988) whenever the overlap is smaller than 10^{-ITOL}. 43 independent k points in the irreducible first Brillouin zone are used in order to calculate the wavefunction: they correspond to the shrinking factor $IS = 8$. These values of the parameters *ITOL* and *IS* are a good compromise between reasonable computational times and sufficient accuracy on the total energy calculations.

In the present study two different atomic orbital (AO) basis sets are adopted to describe the B and N atoms within the crystal: they are termed B_1 and B_2, respectively. The first basis set B_1, of the 6-21G type for both atoms, leads to 18 AO's per unit cell. It has already been used by Orlando *et al.* (1990) to study the diamond-like structures C, BN, SiC, BP, Si and AlP. We have reoptimized the exponents (α) of the outermost shells with respect to the experimental lattice parameter. This process leads to the values $\alpha_{3sp}(B) = 0.1843$ and $\alpha_{3sp}(\mathrm{N}) = 0.3132$, which are close to those obtained by Orlando *et al.* [$\alpha_{3sp}(B) = 0.197$ and $\alpha_{3sp}(\mathrm{N}) = 0.297$] for the optimized geometry. The remaining discrepancy seems to indicate that the curve corresponding to the variations of the unit-cell energy *versus* its volume is flat.

The generality of the results, lattice parameter a_0, bulk modulus B and structure factors F reported in §3 and §4, was proved by the use of a second basis set B_2. Here the B atom is described as in B_1, while the basis set of the N atom is of the 7-311G type. The latter was adjusted by Dovesi, Pisani, Ricca, Roetti & Saunders (1984) for the study of lithium nitride, Li_3N, in which the theoretical structure factors were also calculated and compared successfully with the experimental ones provided by Schulz & Thiemann (1979). In the same way as with B_1, the exponents of the most external Gaussian functions were reoptimized: this leads to $\alpha_{3sp}(\mathrm{B}) = 0.1727$, $\alpha_{3sp}(\mathrm{N}) = 0.4723$ and $\alpha_{4sp}(\mathrm{N}) = 0.2665$. With B_2 the core electrons of the N atom are better described and the valence shell is more expanded compared with B_1. The gain of energy is 120.8 kJ mol^{-1}. The influence of d-like polarization functions was analysed in addition, because they should not be negligible in the calculation of the crystalline orbitals and physical properties (Orlando *et al.*, 1990). In the following they are referred to as B_1^* and B_2^*. The exponent of the single Gaussian-type function is $\alpha_{3d} = 0.8$: it is equal for both atoms and both basis sets.

3. Comparative study of physical properties and electronic charge density

3.1. *Physical properties*

Table 1 reports the equilibrium data obtained with the use of B_1, B_1^*, B_2 and B_2^* basis sets. These data result from the interpolation of the curve $E(V)$ built with 13 energy points with respect to the Murnaghan equation of state (Murnaghan, 1944)

$$E(V) = E_0 + (VB/B')\{[(V_0/V)^{B'}/(B'-1)] + 1\} - V_0B/(B'-1)$$

in the range $(a_0 \pm 0.03)$ Å. It must be noted that the curve $E(V)$ presents a large discontinuity for the a_0 values smaller than $a_0 - 0.03$ Å. This abnormal result occurs in spite of computational cautions, such as the mixing of Fock matrix between two consecutive cycles of the SCF process or the use of the Fock matrix resulting from a previous calculation. It restricts us to explore a small range of the lattice parameter. As a consequence, the accuracy of the bulk modulus (B) and of its derivative (B') is less than usually obtained by this method. By use of B_2^* this difficulty still increases.

Table 1. *Total energy E_0(a.u.); binding energy calculated at the HF level BE_0(a.u.) and corrected for the electronic correlation according to Perdew's formula BE_0 (HF-P; a.u.); lattice parameter a_0 (Å); bulk modulus B (GPa)*

The results of the reference (*c*) are obtained with the use of the B_1* basis set for the optimized geometry.

	B_1	B_1^*	B_2	B_2^*	Exp.	Other theoretical results
E_0	−79.1858	−79.2130	−79.2322	−79.2540	-	−79.2130[a] −79.2500[b]
BE_0	0.326	0.354	0.322	0.344	-	0.3537[a] 0.3250[b] 0.3346[c]
BE_0(HF-P)	-	0.496	-	0.479	0.498[d]	0.4963[a] 0.4817[c]
a_0	3.637	3.619	3.625	3.615	3.615[e]	3.619[a] 3.620[c]
B	402	416	354	-	367[d]	416[a] 416[c]

(*a*) Orlando *et al.* (1990); (*b*) Euwema *et al.* (1974); (*c*) Causà *et al.* (1991); (*d*) Wentzcovitch *et al.* (1986); (*e*) Will *et al.* (1986).

Using B_2 the percentage error of the bulk modulus is estimated to be ~10%.

The binding energy (BE_0) of c-BN is calculated with respect to the free B and N atoms, taken as a reference and described with the same basis sets as in the BN crystal. To take the electronic correlation into account, Perdew's formula (Perdew & Wang, 1991; Perdew, Chevary, Vosko, Pederson, Singh & Fiolhais, 1992) was used as deduced from the density functional theory (DFT) and recently implemented in the *CRYSTAL* code (Causà & Zupan, 1994). The respective results obtained at the Hartree–Fock level (BE_0) and with the correlation-only correction [BE_0(*HF-P*)] are additionally given in Table 1.

For comparison, other theoretical results obtained with the same method are also given in Table 1. The used basis sets are either an effective core pseudopotential set (Causà, Dovesi & Roetti, 1991) or all-electron sets (Orlando *et al.*, 1990; Euwema *et al.*, 1974). A detailed discussion of the effect of the atomic orbital basis sets on the amount of physical properties (E_0, BE_0, a_0, B) is given in the original paper of Orlando *et al.* (1990). A comparison of our results (B_2 and B_2^*) with those of Orlando *et al.* (1990) and Euwema *et al.* (1974) confirms the main outcome of Orlando *et al.* (1990). It will be noted that the use of a more extended basis set (B_2: 7-311 G) in this work instead of B_1 (6-21G) for nitrogen leads to results closer to experiment (Wentzcovitch, Chang & Cohen, 1986). Of course, the total energy E_0 is stabilized by ~0.04 a.u., but the binding energy is slightly deteriorated.

3.2. *Electronic structure and charge density*

The results obtained using B_2 and B_2^* basis sets are compared with those of B_1 and B_1^* in terms of Mulliken population analysis (total atomic charges and overlap populations: Table 2). The figures representing band structure with its associated density of states and the total electron charge-density maps are similar to those published by Orlando *et al.* (1990). For this reason, they are not presented in this work, except some difference charge-density maps, which were determined by inverse Fourier transform of the structure factors (see §4).

Table 2. *Electronic distribution corresponding to a Mulliken population analysis: total charges on the atoms (first two lines) and overlap populations between nearest neighbours (B—N) and second neighbours (B—B and N—N)*

The contribution of *d* orbitals to the total charges is given in parentheses: all the charges are in electrons. Static structure factors F_o, *hkl* are associated with the first nine reflections (last nine lines)

	B_1	B_1^*	B_2	B_2^*
B	3.988	4.147	3.890	4.153
		(0.078)		(0.071)
N	8.012	7.853	8.110	7.847
		(0.022)		(0.023)
B—N	0.528	0.590	0.368	0.510
B—B	−0.001	−0.002	0.003	0.006
N—N	−0.022	−0.017	−0.029	−0.019
111	19.812	19.904	19.840	19.930
200	6.072	6.036	6.120	6.095
220	16.392	16.384	16.456	16.444
222	1.659	1.825	1.716	1.865
F_o, 311	10.100	9.992	10.148	10.043
331	8.769	8.868	8.816	8.908
400	12.717	12.683	12.792	12.751
420	1.016	1.027	1.074	1.079
422	11.436	11.452	11.471	11.482

Examination of Table 2 indicates the semi-covalent character of c-BN, since the charge transfer from B towards N is practically equal to unity and the overlap population between the nearest-neighbour B and N atoms is ~0.5 e. Antibonding forces between second neighbours are very slightly prevailing. Table 2 also indicates that the values are not basis-set-dependent, except the B—N overlap population, which is smaller when calculated with B_2 rather than with B_1. The values

of the B—B populations become positive with B_2 and B_2^*, but remain very small.

The addition of *d*-like polarization functions on B and N atoms increases the covalent character of the compound and especially the population of the B atom.

Further information is obtained by the partition of the electronic charge distribution into atomic multipoles (up to hexadecapole: $l = 4$). This is performed according to a Mulliken scheme and to the definitions given by Saunders, Freyria-Fava, Dovesi, Salasco & Roetti (1992). The atomic spheropoles calculated with B_1^* and B_2^* are 4.00 and 3.94 a.u. for nitrogen and 2.93 and 3.10 a.u. for boron, respectively. These values are practically basis-set-independent. On the other hand, the first non-zero multipoles correspond to the octopole moments ($l = 3, m = 2$); they are rather different when obtained with B_1^* and B_2^* (−16.4 and −7.4 a.u. for N, respectively, and 2.3 and 9.1 a.u. for B, respectively). Negative octopole populations show a loss of electrons near the N atom. The populations of the hexadecapole moments ($l = 4, m = 0$) are associated with the interactions between next-nearest-neighbour atoms. The values obtained (0.46 a.u. for N and −5.52 a.u. for B using B_2^*) prove the existence of this interaction. However, it is not reasonable to discuss the high-order multipoles quantitatively, because they are basis-set-dependent. This seems due to a larger weight associated with the tails of the functions, which constitute their most arbitrary part.

4. Structure factors and electronic charge density

4.1. *Static study*

From the wavefunction calculated at the Hartree–Fock (HF) level, the static electron density $\rho_0(\mathbf{r})$ is deduced by the relationship (Pisani *et al.*, 1988)

$$\rho_0(\mathbf{r}) = \sum_{\mathbf{g}} \sum_{\mu,\nu} P^{\mathbf{g}}_{0_{\mu\nu}} \chi^0_\mu(A, \mathbf{r}) \chi^{\mathbf{g}*}_\nu(B, \mathbf{r}), \qquad (1)$$

where $\chi^0_\mu(A, \mathbf{r})$ is the μth AO on atom $A(\mathbf{r}_A)$ in the origin cell, $\chi^{\mathbf{g}}_\nu(B, \mathbf{r})$ is the νth AO on atom $B(\mathbf{r}_B)$ in the crystal cell associated with the translation vector $\mathbf{g}$ and $P^{\mathbf{g}}_{0_{\mu\nu}}$ is the corresponding element of the density matrix.

The electron charge-density map projected onto the plane perpendicular to the [110] direction is given by Orlando *et al.* (1990) with the use of the B_1^* basis set.

The X-ray structure factors $F_0(\mathbf{s})$ can be calculated from the Fourier transform of the static electron density (Ferrero, 1981)

$$F_0(\mathbf{s}) = \sum_{\mathbf{g}} \sum_{\mu,\nu} P^{\mathbf{g}}_{0_{\mu\nu}} I^{\mathbf{g}}_{0_{\mu\nu}}(\mathbf{s}), \qquad (2a)$$

where the static scattering integral $I^{\mathbf{g}}_{0_{\mu\nu}}(\mathbf{s})$ is developed on the basis of the atomic orbitals. Its expression for the s_x component of the scattering vector $\mathbf{s}$ is given by

$$I^{g_x}_{0\alpha\beta}(s_x) = \int_{-\infty}^{+\infty} (x - x_A)^n e^{-\alpha(x-x_A)^2} (x - x_B - g_x)^m \times e^{-\beta(x-x_B-g_x)^2} e^{-is_x x}\, dx, \qquad (2b)$$

where α and β are exponents of the Gaussian-type functions (GTF's) used in the development of χ_μ and χ_ν AO's: n and m are the degrees of the x polynomial depending on the nature of the encountered AO's. The calculation of this integral was carried out analytically (Ferrero, 1981).

The structure factors of 76 reflections given in Table 3 are calculated by means of (2*a*) and (2*b*) using the four AO basis sets (B_1, B_1^*, B_2 and B_2^*). In general, $F(B_1)$, $F(B_1^*)$, $F(B_2)$ and $F(B_2^*)$ are similar, even in the region of small $(\sin\theta/\lambda)$ values where the basis set effects are expected to be the most sensitive (Table 2). This is also valid when a polarization function is added on a single atom (B or N) with a GTF exponent varying between 0.4 and 0.8. In order to illustrate the basis set effect, the difference $A = F_0(B_2^*) - F_0(B_1^*)$ calculated as a function of $(\sin\theta/\lambda)$ is shown in Fig. 1 (symbol □). As expected, only the first nine reflections show small but significant differences (see also Table 2). The positive values of this difference indicate that the use of B_2^* basis sets leads to a c-BN slightly more ionic than described with B_1^* (see §5). Among them, the two reflections 222 and 420 belonging to the group $h + k + l = 4n + 2$ only show a percentage deviation greater than 1%. This is not surprising, because the corresponding structure factors have a small absolute amount and are very sensitive to the reorganization of the charge density.

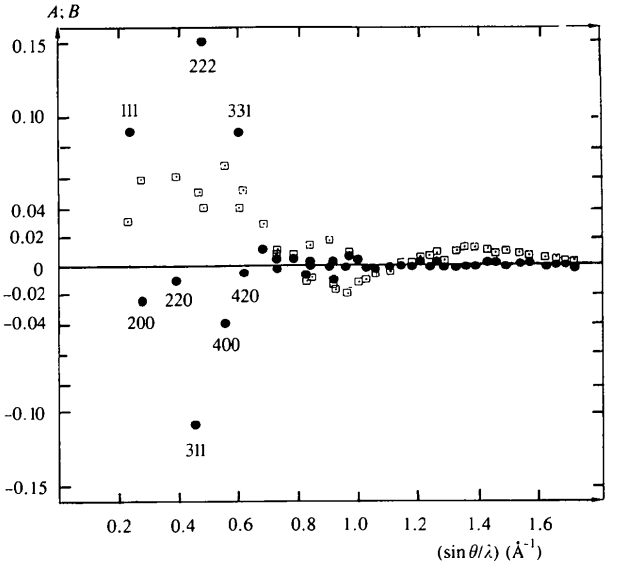

Fig. 1. Influence of the AO basis set upon the values of the static structure factors F_0 *versus* $(\sin\theta/\lambda)$. The symbols ⊡ and ● correspond to the differences $A = F_0(B_2^*) - F_0(B_1^*)$ and $B = F_0(B_2^*) - F_0(B_2)$, respectively.

Table 3. *Static F_0, F_0^{IAM} and dynamic F_T ($T = 298$ K) structure factors of cubic boron nitride calculated with equations (2), (3) and (5), respectively, using the B_2^* basis set*

The values of the experimental lattice parameter $a_0 = 3.615$ Å and temperature factors $B_B = 0.216$, $B_N = 0.178$ and $B_B = 0.204$, $B_N = 0.166$ Å^2 reported by Will *et al.* (1986) and Eichhorn *et al.* (1991) are adopted for the calculations of F_T (*a*) and F_T (*b*) (column 5), respectively. The experimental structure factors (at $T = 298$ K), F_{exp} [*a*] and F_{exp} [*b*], correspond to Josten's (1985) and Eichhorn *et al.*'s (1991) data, respectively.

				F_T			
h k l	$(\sin\theta/\lambda)_0$	F_0	F_0^{IAM}	(*a*)	(*b*)	F_{exp} [*a*]	F_{exp} [*b*]
1 1 1	0.2396	19.930	18.118	19.719	20.232	20.07	18.93
2 0 0	0.2766	6.095	5.338	6.036	5.924	6.35	5.79
2 2 0	0.3912	16.444	16.255	15.949	16.024	16.40	15.80
2 2 2	0.4791	1.865	1.748	1.842	1.980	1.92	1.88
3 1 1	0.4587	10.043	10.379	9.628	9.496	10.10	9.65
3 3 1	0.6029	8.908	8.760	8.304	8.380	8.38	8.34
3 3 3	0.7187	7.758	7.899	7.017	7.036	7.13	7.05
4 0 0	0.5533	12.751	12.970	11.996	11.936	12.13	12.02
4 2 0	0.6186	1.079	1.089	1.079	1.100	1.19	1.16
4 2 2	0.6776	11.482	11.524	10.495	10.548	10.56	10.55
4 4 0	0.7824	10.465	10.531	9.288	9.352	9.33	9.40
4 4 2	0.8299	1.273	1.203	1.223	1.240	1.21	1.22
4 4 4	0.9583	8.915	9.020	7.461	7.540	7.41	7.57
5 1 1	0.7187	7.852	7.899	7.103	7.144	7.08	7.13
5 3 1	0.8183	7.195	7.270	6.325	6.368	6.33	6.39
5 3 3	0.9070	6.708	6.746	5.732	5.792	5.67	5.82
5 5 1	0.9877	6.226	6.288	5.170	5.232	5.14	5.25
5 5 3	1.0624	5.798	5.880	4.680	4.740	4.67	4.78
5 5 5	1.1978	5.116	5.180	3.904	3.972	3.87	4.03
6 0 0	0.8299	1.259	1.203	1.210	1.232	1.22	1.23
6 2 0	0.8748	9.617	9.723	8.287	8.356	8.21	8.38
6 2 2	0.9175	1.395	1.333	1.303	1.324	1.28	1.30
6 4 0	0.9974	1.489	1.436	1.354	1.376	1.33	1.36
6 4 2	1.0350	8.285	8.396	6.735	6.820	6.69	6.84
6 4 4	1.1406	1.590	1.556	1.370	1.396	1.35	1.38
6 6 0	1.1736	7.222	7.330	5.539	5.632	5.59	5.71
6 6 2	1.2058	1.610	1.582	1.350	1.376	1.31	1.36
6 6 4	1.2975	6.357	6.457	4.602	4.696	4.57	4.74
6 6 6	1.4374	1.573	1.558	1.187	1.220	1.16	1.20
7 1 1	0.9877	6.212	6.288	5.158	5.216	5.13	5.23
7 3 1	1.0624	5.810	5.880	4.689	4.752	4.70	4.78
7 3 3	1.1321	5.436	5.512	4.266	4.332	4.23	4.38
7 5 1	1.1978	5.109	5.180	3.898	3.964	3.85	4.00
7 5 3	1.2601	4.814	4.878	3.572	3.640	3.56	3.68
7 5 5	1.3762	4.288	4.350	3.009	3.080	3.01	3.13
7 7 1	1.3762	4.290	4.350	3.010	3.080	2.99	3.13
7 7 3	1.4307	4.060	4.118	2.771	2.840	2.75	2.89
7 7 5	1.5340	3.658	3.709	2.362	2.440	2.36	-
7 7 7	1.6770	3.158	3.202	1.876	1.940	1.91	-
8 0 0	1.1065	7.721	7.835	6.096	6.184	5.96	6.25
8 2 0	1.1406	1.589	1.556	1.369	1.396	1.35	1.39
8 2 2	1.1736	7.220	7.330	5.538	5.628	5.52	5.70
8 4 0	1.2371	6.768	6.872	5.043	5.136	5.03	5.19
8 4 2	1.2677	1.615	1.592	1.319	1.348	1.28	1.33
8 4 4	1.3552	5.984	6.079	4.208	4.300	4.20	4.37
8 6 0	1.3831	1.594	1.577	1.235	1.268	1.16	1.26
8 6 2	1.4105	5.643	5.733	3.856	3.948	3.84	4.01
8 6 4	1.4897	1.547	1.533	1.137	1.172	1.11	-
8 6 6	1.6130	4.539	4.612	2.765	2.852	2.77	-
8 8 0	1.5648	4.782	4.859	2.998	3.088	3.03	-
8 8 2	1.5891	1.485	1.474	1.036	1.072	1.01	-
8 8 4	1.6598	4.315	4.384	2.554	2.640	2.57	-
9 1 1	1.2601	4.810	4.878	3.569	3.638	3.56	3.69
9 3 1	1.3194	4.537	4.602	3.274	3.344	3.23	3.38
9 3 3	1.3762	4.290	4.350	3.010	3.080	3.03	3.13
9 5 1	1.4307	4.061	4.118	2.772	2.840	2.75	2.89
9 5 3	1.4832	3.851	3.905	2.556	2.624	2.53	-
9 5 5	1.5831	3.479	3.527	2.184	2.252	2.20	-
9 7 1	1.5831	3.478	3.527	2.184	2.252	2.20	-
9 7 3	1.6307	3.313	3.358	2.023	2.088	2.03	-

Table 3 (*cont.*)

$h\,k\,l$	$(\sin\theta/\lambda)_0$	F_0	F_0^{IAM}	F_T (*a*)	F_T (*b*)	F_{exp} [*a*]	F_{exp} [*b*]
10, 0 0	1.3831	1.594	1.577	1.235	1.268	1.18	1.25
10, 2 0	1.4105	5.642	5.733	3.856	3.948	3.82	4.03
10, 2 2	1.4374	1.573	1.558	1.187	1.220	1.16	1.20
10, 4 0	1.4897	1.546	1.533	1.137	1.172	1.14	-
10, 4 2	1.5151	5.045	5.126	3.255	3.344	3.27	-
10, 4 4	1.5891	1.485	1.474	1.036	1.072	1.01	-
10, 6 0	1.6130	4.539	4.612	2.765	2.852	2.79	-
10, 6 2	1.6365	1.451	1.441	0.986	1.020	0.98	-
10, 6 4	1.7052	4.107	4.173	2.363	2.448	2.40	-
11, 1 1	1.5340	3.657	3.709	2.361	2.429	2.34	-
11, 3 1	1.5831	3.478	3.527	2.184	2.252	2.18	-
11, 3 3	1.6307	3.312	3.358	2.023	2.088	2.03	-
11, 5 1	1.6770	3.158	3.202	1.876	1.941	1.89	-
12, 0 0	1.6598	4.315	4.384	2.554	2.460	2.59	-
12, 2 0	1.6826	1.416	1.407	0.938	0.972	0.94	-
12, 2 2	1.7052	4.107	4.173	2.363	2.448	2.40	-

In the same way, the effect of the polarization functions can be discussed from the $B = F_0(B_2^*) - F_0(B_2)$ difference values represented in Fig. 1 by the symbol (●). Once again, the first reflections $[(\sin\theta/\lambda) < 0.7\,\text{Å}^{-1}]$ have significant differences which can be either positive (111, 222 and 331) or negative (311 and 400). Since the value of the structure factors of the 111 and 222 reflections measure the asphericity of the valence electron cloud along the [111] direction and the asphericity plus the charge transfer between next neighbours, respectively, the large positive differences associated with these two reflections indicate that the addition of a *d*-like polarization function of the AO basis set increases the covalent character of c-BN. The negative difference of the 311 reflection is large and due to monopole deformation of the atomic wavefunctions. For all the other reflections, the influence of the *d* functions is random and very small. In a previous study of crystalline silicon, Pisani, Dovesi & Orlando (1992) have noted that the addition of one or two *d*-like polarization functions in the AO basis set provides an increase of the 222 structure factor, but the best agreement with respect to experiment (Spackman, 1986) is surprisingly obtained with the use of only one *d* function.

The same kind of observations can be carried out from the results obtained with the couples of basis sets $B_2 - B_1$ and $B_1^* - B_1$. Taking these similarities into account, the structure factors and the electronic charge densities only calculated with the B_2^* basis set are reported in the following.

Our $F_0(\mathbf{s})$ values (column 3 of Table 3), when compared with those calculated by Euwema *et al.* (1974) from the HF method and using a Huzinaga's basis set, are in good agreement. The factor of agreement defined by $R = (\sum_{hkl} |F_0 - F_{Euw}| / \sum_{hkl} F_{Euw})$ is only 0.01. It underlines the quality of the agreement since the nine calculated reflections, which include 222, belong to the valence region very sensitive to the basis set effects.

To discuss the deformation of the electron clouds around the atoms, it is convenient to compare the structure factors of Table 3 (column 3) with those calculated in IAM developed by assimilating the crystal to a superimposition of free atoms. For the zinc blende-type structure, the expressions of the structure factors $F_0^{IAM}(\mathbf{s})$ are given by

$$F_0^{IAM}(\mathbf{s}) = 4[f_{0.B}(\mathbf{s}) + f_{0.N}(\mathbf{s})] \quad \text{for} \quad h+k+l = 4n; \tag{3a}$$

$$F_0^{IAM}(\mathbf{s}) = 4[f_{0.B}(\mathbf{s}) - if_{0.N}(\mathbf{s})] \quad \text{for} \quad h+k+l = 4n+1; \tag{3b}$$

$$F_0^{IAM}(\mathbf{s}) = 4[f_{0.B}(\mathbf{s}) - f_{0.N}(\mathbf{s})] \quad \text{for} \quad h+k+l = 4n+2; \tag{3c}$$

$$F_0^{IAM}(\mathbf{s}) = 4[f_{0.B}(\mathbf{s}) + if_{0.N}(\mathbf{s})] \quad \text{for} \quad h+k+l = 4n-1. \tag{3d}$$

$F_0^{IAM}(\mathbf{s})$ is calculated using both the values of the atomic scattering factors $f_0(\mathbf{s})$ given by *International Tables for Crystallography* (1992, Vol. A) and also the values deduced from the wavefunction of the free atoms described with the same AO basis set (B_2^*) as for the bulk. The corresponding calculated differences $F_0 - F_0^{IAM}$ represented by the symbols ● and ▼, respectively, are reported *versus* $(\sin\theta/\lambda)$ in Fig. 2.

Examination of Fig. 2 shows clearly two results: (i) the first concerns the basis set effect, which is significant only for the first five reflections identified on this figure. Therefore, they are the most sensitive to the quality of the description of the valence charge and are very appropriate to discuss the deformation of the electron clouds. (ii) The second result corresponds to the deviation of the differences $F_0 - F_0^{IAM}$ with respect to the zero line. It is significant for the identified (Fig. 2) seven reflections and especially for 111 and 200. The

largest positive difference is associated with the 111 reflection. It contains both the contributions of B and N atoms and represents 8% of the F_0(s) value. It also expresses the deformation of the electron clouds of both atoms along the [111] direction and is correlated in part to the covalent character of the B—N bond. Whereas the 200 reflection is controlled by the charge transfer alone, the amount of the 222 reflection describes again the asphericity of the charge density, but also the charge transfer from the B to the N atom. The negative value of $F_0 - F_0^{IAM}$ corresponding to the 311 and 400 reflections can be explained by the monopole deformation of atomic wavefunctions in comparison to the free state. Similar features are known from the electron distribution in diamond (Spackman, 1991).

The previous results are also illustrated by the difference electron charge-density (DECHD) maps, which are obtained by the Fourier sum of the structure-factor differences $F(B_2^*) - F^{IAM}(B_2^*)$ (Pietsch, Tsirelson & Ozerov, 1986). In F^{IAM}, the overlap between neighbouring atoms is neglected. Since both $F(B_2^*)$ and F^{IAM} are complex, no phase error appears. The DECHD map is projected onto the (110) plane and represented in Fig. 3(*a*), in which the [111], [$\bar{1}$11] and [001] directions are also indicated. As already underlined, there is no significant difference with the map reported by Orlando *et al.* (1990), since it was well established that the results are practically basis independent.

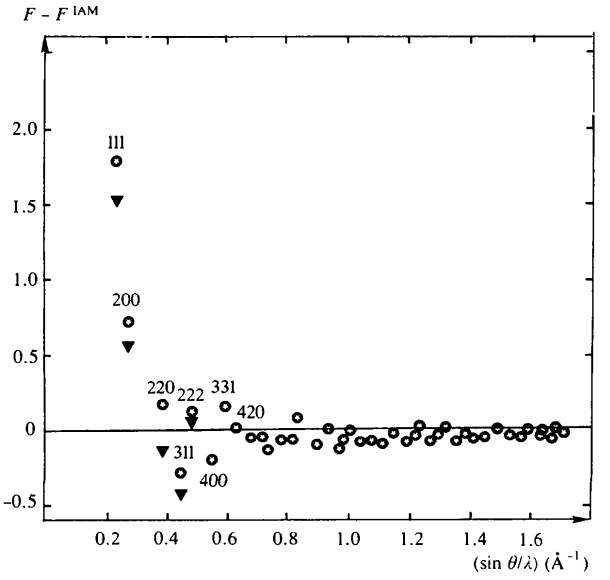

Fig. 2. Variations of the differences $F - F^{IAM}$ *versus* $(\sin\theta/\lambda)$. The symbols ● and ☆ correspond to the B_2^* basis set for the calculation of F and F^{IAM} in the static and dynamic cases, respectively. In this last case, the atomic scattering factors (equations 3) are corrected by the temperature factors $B_B = 0.216$ and $B_N = 0.178\,\text{Å}^2$ (Will *et al.*, 1986). The symbol ▼ corresponds to the static case where F and F^{IAM} are calculated with B_2^* and *International Tables for Crystallography* (1992, Vol. A), respectively.

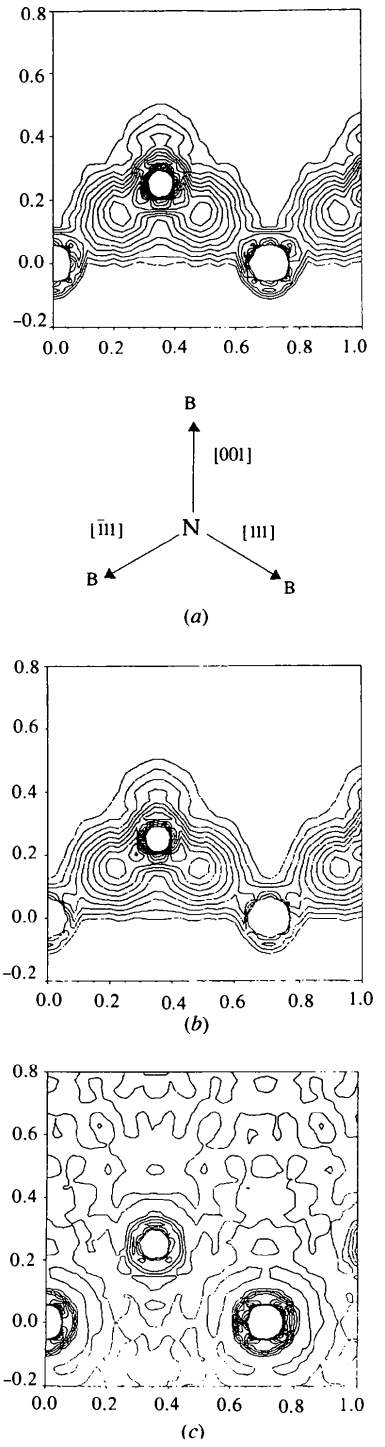

Fig. 3. Difference electron charge-density maps constructed by Fourier sum of the differences $F - F^{IAM}$ and projected onto the plane (110). (*a*) Static density $F_0(B_2^*) - F_0^{IAM}(B_2^*)$; (*b*) dynamic ($T = 298$ K) density $F_T(B_2^*) - F_T^{IAM}(B_2^*)$; (*c*) difference between Figs. 3(*a*) and (*b*). Only the positive contours are given for clarity: the step widths are $0.057\,\text{e Å}^{-3}$ for (*a*) and (*b*), and $0.005\,\text{e Å}^{-3}$ for (*c*).

4.2. *Dynamic study*

A quantum methodology of the calculation of dynamic structure factors at a given temperature T has been developed (Azavant, Lichanot, Rérat & Chaillet, 1994) and recently improved for the study of magnesium difluoride in its rutile structure (Azavant, Lichanot, Rérat & Pisani, 1996). It is based on the Debye theory, supposing that nuclei move independently from each other with a displacement $\mathbf{u}$ around their equilibrium positions according to a probability density function $p(\mathbf{u})$ of Gaussian form within the harmonic approximation (Willis & Pryor, 1975)

$$p(\mathbf{u}) = [\det(B^{-1})/(2\pi)^3]^{1/2}\, e^{-\frac{1}{2}\mathbf{u}^T B^{-1}\mathbf{u}}. \quad (4)$$

The thermal vibrations of each atom are characterized by the mean-square displacements tensor

$$B_{ij} = 8\pi^2\langle u_i u_j\rangle, \quad i,j \equiv x,y,z.$$

Introducing the atomic displacements $\mathbf{u}$ and the probability density functions $p(\mathbf{u})$ in (2*a*) and (2*b*), an expression of the dynamic structure factor $F_T(\mathbf{s})$ can be derived, which is formally identical to the static one (2*a*)

$$F_T(\mathbf{s}) = \sum_{\mathbf{g}}\sum_{\mu,\nu} P^{\mathbf{g}}_{T_{\mu\nu}} I^{\mathbf{g}}_{T_{\mu\nu}}(\mathbf{s}). \quad (5)$$

In order to satisfy the normalization condition $F_T(\mathbf{s}=\mathbf{0}) = n_e$ (n_e = number of electrons per unit cell), a dynamic density matrix P_T is introduced from the static one P_0 by

$$P^{\mathbf{g}}_{T_{\mu\nu}} = P^{\mathbf{g}}_{0_{\mu\nu}} I^{\mathbf{g}}_{0_{\mu\nu}}(\mathbf{s}=\mathbf{0})/I^{\mathbf{g}}_{T_{\mu\nu}}(\mathbf{s}=\mathbf{0}). \quad (6)$$

The dynamic scattering integral $I_T(\mathbf{s})$ brings in modified exponents α^T_{ij} for the GTF's describing the atomic orbitals μ and ν: $\alpha^T_{ij} = \alpha/(1+2\alpha B_{ij})$ (Azavant *et al.*, 1994).

In the studies which led thanks to this methodology, the values adopted for the atomic temperature factors B result from a refinement between the experimental X-ray structure factors and those calculated within the IAM.

In the present study we have adopted at $T = 298$ K the values $B_B = 0.216$, $B_N = 0.178$ and $B_B = 0.204$, $B_N = 0.166$ Å^2. These two couples are derived from the refinement of the data of Will *et al.* (1986) and of Eichhorn *et al.* (1991), respectively, for the high-order reflections. In the zinc blende structure the symmetry site of each atom is $\bar{4}3m$ and assigns isotropic temperature factors. From (5) and (6), $F_T(\mathbf{s})$ were computed and the values obtained with the use of B^*_2 are reported in column 5 of Table 3. For comparison, the experimental values of Josten (1985) and Eichhorn *et al.* (1991) are also given in columns 6 and 7, respectively. The dynamic difference $F_T - F_T^{\mathrm{IAM}}$ is calculated using the same B values to correct the atomic static scattering factors (3) with the Debye–Waller term and reported in Fig. 2 (symbol ☆) for comparison with static differences $F_0 - F_0^{\mathrm{IAM}}$ (symbol ●). The dynamic DECHD (Fig. 3*b*) is deduced by a Fourier sum and projected onto the (110) plane.

4.3. *Temperature effect*

As a preliminary observation, it must be noted that the temperature effect does not modify the precision associated with the basis set effects or with the influence of a polarization function which has been obtained in the static case and presented in Fig. 1.

Examination of Fig. 2 shows that the values of the static (symbols ●) and dynamic (symbols ☆) differences $F - F^{\mathrm{IAM}}$ are the same even in the region of small $(\sin\theta/\lambda)$ values. This result indicates that the deformation of the electron clouds is not altered at this temperature ($T = 298$ K) by the thermal motion, especially along the bond direction [111]. To quantify more precisely this effect, the difference between the static (Fig. 3*a*) and dynamic (Fig. 3*b*) DECHD maps is calculated and projected onto the same plane, (110) (Fig. 3*c*). The concentration of positive isodensity curves around nitrogen shows that the semi-ionic

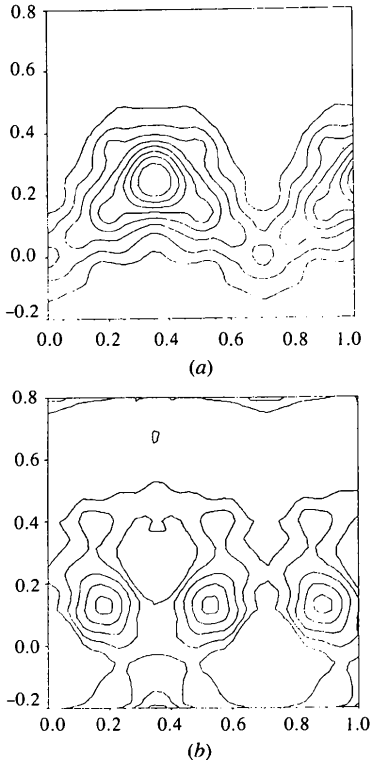

Fig. 4. Refined difference electron charge density constructed by Fourier sum of experimental structure amplitudes obtained at $T = 298$ K. (*a*) Contours obtained from Josten's (1985) data (76 reflections; $B_B = 0.233$, $B_N = 0.184$ Å^2); (*b*) contours obtained from Eichhorn *et al.*'s (1991) data (52 reflections; $B_B = 0.204$, $B_N = 0.166$ Å^2). The step widths are 0.057 e Å^{-3} for (*a*) and (*b*).

character of c-BN is stronger in the static case than in the dynamic one. In other words, the 0.8 e charge transfer from boron to nitrogen calculated at 0 K by Mulliken population analysis becomes smaller at $T = 298$ K. This result is closer to the results of Will *et al.* (1986). Unfortunately, it is not possible to quantify this new charge transfer, since the dynamic density matrix still cannot be calculated and the Mulliken population deduced.

4.4. *Comparison with experiments*

The examination of experimental and theoretical data reveals a fairly good agreement beyond the 420 reflection. The six low-order reflections calculated with the B_2^* basis set are generally lower or larger compared with the experimental values reported by Josten (1985) and Eichhorn *et al.* (1991), respectively. Thus, the general discrepancy between both experimental data sets cannot be removed by theory. It must be noted that the use of the B_2^* set generally leads to a better R-agreement factor. With respect to Josten's data, for example, the value of the agreement factor defined by $R = \sum_{hkl} |F_{calc} - F_{exp}| / \sum_{hkl} F_{exp}$ is 0.012 (9), while it becomes 0.015, 0.0144 and 0.0133 with B_1, B_1^* and B_2, respectively. With respect to Eichhorn *et al.*'s (1991) data, the R factor corresponding to B_2^* is only 0.0145. High-order reflections explain the poorer agreement with Eichhorn's data. The number of reflections considered in the refinement of the atomic mean-square displacements is smaller than in Josten's data and certainly leads to less accurate B values in that case. For simplification, the B values given by Josten are only used in the following. A qualitative inspection of the experimental data can be given on the level of the constructed difference densities $|F_{exp} - F^{IAM}|$. It was performed by a similar procedure, as reported in Pietsch *et al.* (1986). For simplification, similar phases were used for F_{exp} and F^{IAM} and the respective density plots are shown in Figs. 4(*a*) and (*b*). It can be noted that the influence of a slight change of B_B and B_N on the respective difference densities is small and does not change the features, qualitatively. Whereas the density calculated from Josten's data exhibits a charge density accumulation close to the nitrogen site, the plot obtained from Eichhorn's data shows a charge-density maximum between the next neighbours. Qualitatively, similar results were published by the experimentalist who discussed their data on the level of model densities refined by a multipole model.

From a qualitative point of view, the outcome of our calculation is closer to Eichhorn's than to Josten's data. It supports the general assumption that the chemical bond in cubic BN is mainly covalent, but slightly disturbed by the electron charge transfer from boron to nitrogen (semi-covalent bond). Obviously, this charge transfer is known as model-dependent when Josten's and Eichhorn's data are used. Note that our difference densities are calculated from experimental data only, without using a model density and taking into account a small phase error. This gives rise to some quantitative, but not qualitative, disagreements to these densities refined by a multipole model. Quantitatively, the Hartree–Fock density maximum is twice compared with Eichhorn's data. On the other hand, the charge transfer evaluated by Will *et al.* [1986 (0.45 e)] is half that obtained by our Mulliken population analysis (0.8 e). This is in disagreement to our qualitative discussion, but may be explained by conceptional discrepancies (see below).

5. Discussion and concluding remarks

In order to explain the discrepancies between the HF density and the experimental ones, the following comments have to be taken into account.

First, as shown by Josten (1985), for example, the relative position of this saddle point depends on the model of data refinement used. It is located closer to the nitrogen site using a bond charge model or nearer to the boron using a multipole model. This discrepancy documents the general phase problem of the X-ray structure analysis which is most important, even for non-centrosymmetric structures. Because the X-ray experiment provides the amplitudes and not the phases of the structure factors, the experimental data cannot be separated into atomic portions. This also prevents a correct multipole analysis (El Haouzi & Hansen, 1996) and other site-dependent corrections (anomalous dispersion *etc.*). Thus, the charge-density analysis is only possible on the basis of any model and requires other relevant structure assumptions. Similar arguments also hold concerning the refinement of Eichhorn's data.

Second, the theoretical and experimental difference densities are based on different IAM models. Whereas the IAM of *CRYSTAL*92 contains equal deformations of orbitals than those within the crystal, the IAM taken from *International Tables for Crystallography* (1992, Vol. A) is based on the 'free atomic model'. A shrinkage or extension of cores can produce additional features close to the atomic sites, which mimics a twin peak behaviour as found experimentally.

Third, the ionic charge of nitrogen is calculated by the use of different approximations. The experimental procedure given by Will *et al.* (1986) is performed within an 'ionic' radius, which is defined by the position of the minimum charge density between next neighbours. The summarized charge (9.44 e) is lower than 12 e. The difference is equally distributed between both ions. This is incorrect, taking the different screening constants of ionic wavefunctions into account. Thus, the experimental charge density is rather underdetermined.

However, a correct comparison between theory and experiment is possible in terms of structure amplitudes only. As stated above, the low-order reflections calculated by *CRYSTAL* are generally smaller or larger compared with the experiment. Our charge-density maximum amounts to $0.53\,e\,Å^{-3}$, which is larger than that given by Will *et al.* [1986 ($0.3\,e\,Å^{-3}$)] and Eichhorn *et al.* [1991 ($0.23\,e\,Å^{-3}$)]. A similar discrepancy has already been found for diamond. Whereas the HF calculations reveal a peak of $\sim 0.6\,e\,Å^{-3}$, the experimental data give rise to a lower peak maximum between 0.40 and $0.44\,e\,Å^{-3}$ (Spackman, 1986, 1991). On the other hand, the large charge transfer from boron to nitrogen cancels the difference in the ionic radii of the B and N atoms and localizes the bond charge close to the midpoint between next neighbours. Using the charge-density maps given by Orlando *et al.* (1990) the density maximum of c-BN is only slightly lower than that of diamond. The similar hardness and bulk modulus of both compounds may be explained by the fact that the loss of covalency is compensated by the ionicity of c-BN. The important influence of ionicity is even documented by the amount of Debye–Waller factors. Both B_B and B_N are larger than B_C found for diamond [$0.14\,Å^2$ (Spackman, 1991)]. That the Debye–Waller factor increases as a function of ionicity was already found by Schumski, Bublik & Gorelik (1971) and corresponds to the row Ge–GaAs–ZnSe (Pietsch, 1985). The valence charge density of diamond documents a twin peak behaviour in the experimental density (Spackman, 1991), as in the total HF density (Orlando *et al.*, 1990). For a valence density plot of c-BN we would expect similar behaviour. Unfortunately, under the present state of program code it cannot be performed yet.

In summary, we present HF calculations of the X-ray structure amplitudes and the difference charge density for c-BN. Whereas the high-order reflections are well described by theory, discrepancies remains for low-order reflections. This can only be partially explained by conceptional differences of density calculations between experiment and theory.

Financial support from the Human Capital and Mobility Programme of the European Union under contract CHRX-CT93-0155 is gratefully acknowledged.

References

Atake, T., Takai, S., Honda, A., Saito, Y. & Saito, K. (1991). Report of Research Laboratory of Engineering Materials Tokyo Institute of Technology, Vol. 16, pp. 15–23.

Azavant, P., Lichanot, A., Rérat, M. & Chaillet, M. (1994). *Theor. Chim. Acta,* **89**, 213–226.

Azavant, P., Lichanot, A., Rérat, M. & Pisani, C. (1996). *Int. J. Quantum Chem.* **58**, 419–429.

Brookes, C. A., Hooper, R. M. & Lambert, W. A. (1983). *Philos. Mag. A,* **47**, L9–L12.

Causà, M. & Zupan, A. (1994). *Chem. Phys. Lett.* **220**, 145–153.

Causà, M., Dovesi, R. & Roetti, C. (1991). *Phys. Rev. B,* **43**, 11937–11943.

Cohen, M. L. & Chelikowsky, J. R. (1989). *Electronic Structure and Optical Properties of Semiconductors.* Berlin: Springer-Verlag.

Dovesi, R., Pisani, C., Ricca, F., Roetti, C. & Saunders, V. R. (1984). *Phys. Rev. B,* **30**, 972–979.

Dovesi, R., Pisani, C., Roetti, C., Causà, M. & Saunders, V. R. (1989). *CRYSTAL88.* QCPE, Program 577. Indiana University, Bloomington, Indiana.

Dovesi, R., Roetti, C. & Saunders, V. R. (1992). *CRYSTAL92 User Documentation.* University of Torino, Italy, and SERC Daresbury Laboratory, UK.

Eichhorn, K., Kirfel, A., Grochowski, J. & Serda, P. (1991). *Acta Cryst.* B**47**, 843–848.

El Haouzi, E. & Hansen, B. (1996). *Acta Cryst.* Submitted.

Euwema, R. N., Surratt, G. T., Wilhite, D. L. & Wepfer, G. G. (1974). *Philos. Mag.* **29**, 1033–1039.

Ferrero, E. (1981). Thesis. University of Torino, Italy.

Josten, B. (1985). Thesis. University of Bonn, Germany.

Murnaghan, F. D. (1944). *Proc. Natl Acad. Sci. USA,* **30**, 244–247.

Orlando, R., Dovesi, R., Roetti, C. & Saunders, V. R. (1990). *J. Phys. C,* **2**, 7769–7789.

Perdew, J. P. & Wang, Y. (1991). *Phys. Rev. B,* **45**, 13244–13249.

Perdew, J. P., Chevary, J. A., Vosko, S. H., Pederson, M. R., Singh, D. J. & Fiolhais, C. (1993). *Phys. Rev. B,* **46**, 6671–6674.

Pietsch, U. (1985). *Phys. Status Solidi B,* **128**, 439–445.

Pietsch, U., Tsirelson, V. G. & Ozerov, R. P. (1986). *Phys. Status Solidi B,* **138**, 47–52.

Pisani, C., Dovesi, R. & Orlando, R. (1992). *Int. J. Quantum Chem.* **42**, 5–33.

Pisani, C., Dovesi, R. & Roetti, R. (1988). Hartree–Fock *ab initio* treatment of crystalline systems, *Lecture Notes in Chemistry*, Vol. 48. Berlin: Springer-Verlag.

Saunders, V. R., Freyria-Fava, C., Dovesi, R., Salasco, L. & Roetti, C. (1992). *Mol. Phys.* 77, 629–665.

Schulz, H. & Thiemann, K. H. (1979). *Acta Cryst.* A**35**, 309–314.

Schumski, M. G., Bublik, W. T. & Gorelik, S. S. (1971). *Kristallographia,* **16**, 77–83.

Spackman, M. A. (1986). *Acta Cryst.* A**42**, 271–281.

Spackman, M. A. (1991). *Acta Cryst.* A**47**, 420–427.

Takama, T., Tsuchiya, K., Kobayashi, K. & Sato, S. (1990). *Acta Cryst.* A**46**, 514–517.

Weiss, R. J. (1974). *Philos. Mag.* **29**, 1029–1032.

Wentfor, R. H. (1957). *J. Chem. Phys.* **26**, 956–959.

Wentzcovitch, R. M., Chang, K. J. & Cohen, M. L. (1986). *Phys. Rev. B,* **34**, 1071–1079.

Will, G., Kirfel, A. & Josten, B. (1986). *J. Less-Common Met.* **117**, 61–71.

Willis, B. T. M. & Pryor, A. W. (1975). *Thermal Vibrations in Crystallography*, Ch. 4, p. 96. Cambridge University Press.